Journal of Harbin Engineering University
ISSN: 1006-7043

Vol 46 No. 1
january 2025

Investigation of The Effects of Material Extrusion Parameters on The Compressive Properties of Onyxtm Composites Using Honeycomb Lattice Configurations.

Dr . S. Sellakumar
Assistant Profesor, Department of Mechanical Engineering, Saveetha Engineering College, Chennai

Abstract
Honeycomb patterns find extensive use across various fields such as engineering, architecture, and transportation. The rapid development of custom structures is made possible through Digital Manufacturing techniques. This study employs an experimental approach to investigate how different material extrusion (MEX) elements impact the natural and mechanical properties of Triagonal honeycomb lactic-structured composites made of Onyx™. To assess the impact of various Material Extrusion (MEX) parameters on the lattice structure, the study examines changes in density, compressive strength, and structural area deviation by adjusting factors such as infill density, layer height, infill pattern, build orientation, and the number of walls.

To achieve maximum compressive strength, the study identified that the optimal parameters include a layer height of 0.1 mm, an infill density of 50%, a build orientation of 90°, a rectilinear infill pattern, and three walls. These specific settings were found to be the most effective for enhancing compressive strength.The mechanical properties of lattice structures made from Onyx™ composite are primarily affected by infill density, build orientation, and infill pattern. Additionally, structures with three walls exhibit greater resistance to buckling compared to those with one or two walls.This study identifies build direction and layer height as the main factors influencing structural area deviation in integrated lattices.

The paper also presents a topologically optimized lattice-structured bracket designed for maximum load-bearing capacity. This bracket could find applications in sports action cameras, prosthetics, surgical planning, and medical or dental instruments.

Keywords: Onyx™ , Topological Optimization, Triagonal Honeycomb Structures

1. Introduction

Lattice structures are defined by a recurring arrangement of interconnected elements, a characteristic feature in architectural and engineering constructions[1]. The lattice structure's repeating unit cells function as a network that redistributes loads, resulting in lower stress and increased stability under applied stresses[2]. Lattice structures offer superior load-bearing capacity compared to solid designs, despite utilizing less material[3]. Lattice structures find applications across diverse domains such as industrial design, aircraft, civil engineering, automotive engineering, and architecture[4]. Lattice structures are categorized into several classes, including Honeycomb, TPMS, Voronoi, and Beam[5].Honeycomb lattices are known for their exceptional energy absorption capabilities and offer remarkable structural stability. They achieve an advantageous strength-to-weight ratio, making them highly efficient for various applications [6].Triangular lattice structures are highly favored in honeycomb planar lattice arrays for their remarkable structural stiffness, isotropic qualities, higher packing density, scalability, and modularity[7].Traditional manufacturing processes, such as compression molding, face challenges in producing triangular honeycomb lattices due to their intricate geometries. These challenges include achieving precise dimensions, with potential deviations at the micron scale, and the complexity of mold design. Furthermore, these methods limit the design flexibility for such lattices [8].Advances in Additive Manufacturing (AM) allow for the efficient production of lattice structures, offering high design flexibility through the layer-by-layer deposition of materials [9].The strengths of

Additive Manufacturing (AM) include its design flexibility, minimal material waste, rapid prototyping, adaptable production processes, ability to create intricate structures, and efficient repair capabilities [10]. Moreover, the adoption of AM methods has revolutionized production across various sectors, such as consumer products, automotive, aerospace, and healthcare[11].Fused Filament Fabrication (FFF) creates polymer parts by depositing polymeric material layer by layer [12].The FFF approach stands out as the most extensively adaptable Additive Manufacturing (AM) technology, thanks to its remarkable features, including cost-effectiveness, compatibility with a wide variety of materials, improved design flexibility, and user-friendly operation [13].

Polymeric lattice structures are attracting attention because of their enhanced properties, such as a high surface area-to-volume ratio, material efficiency with reduced consumption, lightweight design, and excellent load-bearing capacity [14].This section includes several studies on well-organized polymeric lattice structures. Bello et al. used Digital Image Correlation (DIC) to investigate PLA lattice structures and understand how printing parameters impact their mechanical properties. Their findings indicated that increasing the printing temperature improved tensile properties but led to a trend of decline in yield strength [15]. Günaydın yet al. conducted a study on the energy absorption properties of re-entrant auxetic lattice structures made from ABS. Utilizing both experimental methods and simulation techniques, they discovered that lowering the rotational stiffness at the nodes significantly improved the energy absorption

capacity of these lattices [16]. Patro et al. investigated how 3D printed PLA and ABS honeycomb structures respond to compression at different loading rates. Their findings revealed that the thickness of the cell walls, the material characteristics, and the loading rates all have a substantial impact on the compressive performance of these honeycombs [17].

Polymeric composite materials are extensively used to create highly functional load-bearing components due to their outstanding strength-to-weight ratios and superior energy absorption capabilities [18]. The selection of the polymeric base and reinforcing material significantly influences the enhancement of energy absorption and mechanical strength when using polymeric composite materials for component fabrication [19]. Synthetic fiber-reinforced polymeric composites surpass particle-reinforced ones, demonstrating superior strength and durability among the different types of polymeric composite materials [20].

PLA, ABS, PETG, Nylon (Polyamide), and other similar basic matrix polymers are commonly used in synthetic fiber-reinforced polymeric composite materials [21]. Nylon is an outstanding matrix material due to its superior mechanical properties, such as enhanced toughness and improved synergy with reinforcing fibers. Additionally, its excellent fuse printability and remarkable chemical stability further contribute to its exceptional performance [22]. Buj-Corral et al. examined the dimensional accuracy and form errors of 3D-printed spur gears made from PLA and nylon. Their findings indicate that nylon gears, when printed with lower infill densities, exhibit fewer form errors compared to PLA gears [23].

Andrey et al. demonstrated that nylon surpasses ABS in the fatigue performance of 3D printed parts, particularly at elevated stress levels, as indicated by a steeper fatigue response curve. Furthermore, they discovered that the tri-hexagon internal shape maximizes fatigue life [24]. In their study investigating the printability and functionality of additive manufactured nylon components, Makki et al. determined that the optimal temperature range for achieving the best mechanical and thermal properties was between 250°C and 255°C. They also confirmed that exceeding this range negatively affected the printed parts, resulting in reduced stiffness and strength [25].

Carbon fiber is notable for its high stiffness-to-strength ratio, setting it apart from other reinforcements such as rayon, polyester, glass, and Kevlar. This characteristic makes it ideal for applications requiring weight reduction, improved dimensional stability, and enhanced electrical and thermal properties [26]. Onyx™, a composite filament made from nylon and reinforced with chopped carbon microfibers, provides exceptional

strength, wear resistance, toughness, and an excellent surface finish. These qualities have spurred extensive research into its potential for 3D printing applications [27].

Peng et al. investigated energy absorption in polyamide composites reinforced with a combination of short and continuous carbon fibers. They determined that a ±45° continuous fiber raster angle was optimal, yielding a high energy absorption value of 1613.3 MJ/mm³.Vidakis et al. utilized the melt extrusion process to modify polyamide 12 (PA12) with carbon black (CB), producing nanocomposite filaments. They found that a 5% concentration of carbon black enhanced the properties of the polyamide nanocomposite, as evidenced by improvements in its mechanical and electrical characteristics. These composites were deemed suitable for developing flexible sensors and circuitry [29].Similarly, Vidakis et al. reinforced polyamide with multiwalled carbon nanotubes (CNTs) to create a nanocomposite and investigated its electrical and antibacterial properties. Their results aligned with prior research, indicating that mechanical properties

are enhanced by multiwalled CNTs at a 5% concentration, while antibacterial activity is not observed at an elevated concentration of 10% wt% [30].

Carbon fiber-reinforced lightweight composite lattices are gaining considerable attention in aerospace, civil, and mechanical engineering fields due to their high versatility and superior performance [31]. Composite lattices reinforced with carbon fiber demonstrate exceptional specific strength, impressive impact resistance, and enduring corrosion resistance [32]. Carbon fiber composites offer superior mechanical properties and improved energy absorption compared to pure polymeric lattices [33]. Although research efforts are limited, numerous studies have investigated the development of composite lattice structures reinforced with carbon fiber. For example, Andrew et al. focused on the development of CF/PEEK cellular materials and assessed their ability to absorb energy and self-sense. Research has shown that CF/PEEK lattices exhibit piezoresistive behavior under both in-plane and out-of-plane compressional loading, indicating their potential use as strain sensors. Additionally, these studies emphasize the role of CF/PEEK lattices in creating lightweight materials with excellent compressive strength[34]. Moreno et al. explored the use of carbon and glass fiber reinforcements in Onyx™, utilizing a multi-directional laminate configuration. Their research indicates a positive relationship between the number of reinforcement layers and tensile strength [35].

In Fused Filament Fabrication (FFF) additive manufacturing, Material Extrusion (MEX) parameters play a critical role in determining the dimensional accuracy, porosity, and interlayer adhesion of carbon fiber composites. These factors, in turn, significantly affect the mechanical properties and energy absorption capabilities of the printed structures. Current research aims to optimize these parameters to enhance the performance of reinforced lattice structures.

Ali et al. discovered that increasing the infill density and utilizing rectangular infill patterns enhanced the tensile strength of 3D-printed Onyx™ composites reinforced with carbon fiber [36]. Nikiema et al. investigated how humidity and various printing settings influence the mechanical properties of additively manufactured Onyx™ composites. Their study revealed a 10% fluctuation in mechanical properties depending on the orientation of the prints [37].

The mechanical properties of carbon fiber-reinforced lattices influenced by MEX factors are still largely unexplored. In their research, Vijayakumar et al. analyzed the impact of process parameters on the mechanical integrity and dimensional precision of PETG composites reinforced with carbon fibers, specifically configured in a hexagonal lattice design. They discovered that samples produced at a temperature of 220°C demonstrated enhanced strength and maintained better dimensional accuracy [38]. Gong et al. developed a microwave absorber utilizing a honeycomb lattice structure through additive manufacturing, employing a polyamide composite reinforced with carbon fiber. The resulting Functional Honeycomb Structural Absorber (FHSA) demonstrated broadband absorption spanning 13.2 GHz and exhibited a minimal reflection loss of -47 dB at 16.2 GHz, even

when subjected to a significant bending angle of 150 degrees [39].

This research examines how various MEX parameters, such as wall count and layer height, influence the mechanical and physical attributes, including diameter deviation, density, and compressive strength, of 3D-printed triangular lattices made from Onyx™ carbon fiber-reinforced polyamide composite. The objective is to determine the ideal MEX settings for producing camera brackets utilizing this lattice structure.

2. Experimental Methodology:

2.1. Materials Used:

In this study, lightweight lattice-structured components were fabricated using Onyx™, a composite material consisting of micro-carbon fiber-reinforced nylon. This composite material is chosen for its exceptional chemical resistance, durability, and strength. Key characteristics of Onyx™ include a tensile strength of 33.5 MPa, a density of 1.2 g/cm³, an elastic modulus of 1.4 GPa, and a Poisson's ratio of 0.35. The specific Onyx™ filament and the FFF (Fused Filament Fabrication) printer used in this research are depicted in Figure 1.

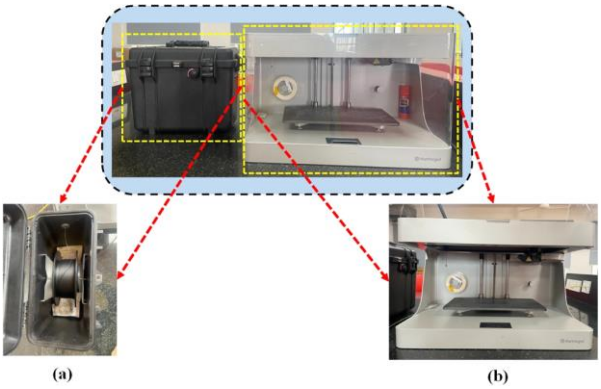

Fig. 1. (a) Onyx™ composite filament, (b) Mark Two 3D printer.

2.2 Lattice-Structured Composites Design:

An Onyx™ compression composite was designed with a diameter of 12.7 mm and a height of 25.4 mm, following the specifications of ASTM D695. This initial solid model was created using nTopology CAD software. To enhance the structure, a triangular planar lattice with unit cells measuring 3 mm and a thickness of 1 mm was incorporated into the solid model, resulting in the final lattice-structured Onyx™ compression composite. The completed CAD model is depicted in Figure 2.

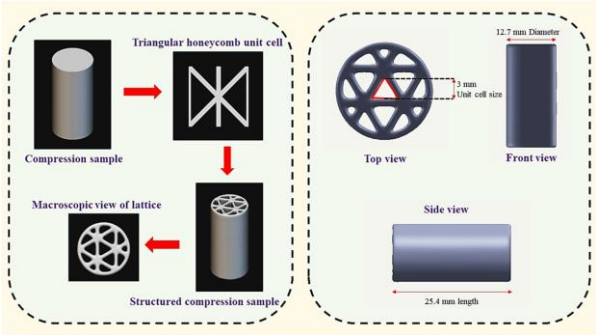

Fig. 2. Modeling of Onyx™ compression composites with a triangular planar-based lattice structure.

2.3. Manufacturing Lattice-Structured Composites:

Onyx™ compression composites with a lattice structure are produced through additive manufacturing. The process begins with converting a CAD model into an STL file. This file is then sliced into G-code using software such as Eiger or Markforged. The resulting G-code is uploaded to a Markforged Mark Two or Desktop 3D printer for Fused Filament Fabrication (FFF) production.

Table 1
Choosing Levels for MEX Factors.

Sl. No	MEX factors	Levels		
1.	Layer height (mm)	0.1	0.2	0.3
2.	Infill density (%)	30	40	50
3.	Build orientation (°)	0	45	90
4.	Infill pattern	Triangle	Hexagon	Rectilinear
5.	Number of walls	1	2	3

The mechanical and physical properties of the produced composites are greatly affected by MEX parameters. Standard MEX settings included a line width of 0.1 mm, an infill flow rate of 100%, a print speed of 20 mm/s, and a print temperature of 275 °C. To examine the impact of individual MEX factors, each parameter was independently varied while keeping the others constant. A key variable, build orientation, was analyzed at angles of 0°, 45°, and 90° relative to the build bed.

2.4. Analyzing the Physical and Mechanical Attributes of Lattice-Structured Composites.

After production, the physical and mechanical properties of the triangular lattice Onyx™ composites were assessed using various techniques. The evaluation focused on the lattices' characteristics, including diameter, density, structural area, and compressive strength. Figure 3 presents a graphical representation of these properties.

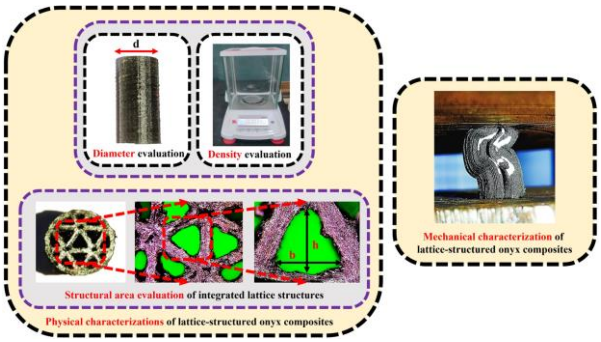

Fig. 3. Characterization of Physical and Mechanical Properties of Lattice-Structured Onyx™ Composites.

2.4.1. Evaluation of Compressive Strength in Developed Composites

The compressive strength of triangular lattice Onyx™ composites was assessed using a Tinus Olsen Universal Testing Machine (UTM) with a 50 kN capacity, in accordance with ASTM D695 standards. Testing involved compressing samples at a rate of 1 mm/min, with the axial load applied along the length of the samples. Each test was conducted in quintuplicate to ensure data reliability. The average compressive strength was then computed for analysis.

2.4.2. Assessment of the density in lattice-structured composites.

The density of triangular planar Onyx™ compression composites was determined using a Pioneer PX125D semi-micro balance, which boasts an accuracy of 1×10-5 g. The mass of each composite was meticulously recorded, and its volume was calculated using CAD software. The density, represented by ρ, was then calculated using the formula

$$\rho = m/v, \quad (1)$$

where m is the mass and v is the volume. To ensure precision, the density values were averaged from five separate mass measurements for each composite. This comprehensive density measurement was subsequently utilized to analyze the impact of various MEX variables on the density variations within the lattice structure.

2.5. Characterization of structural properties.

The research methodology was centered on the mechanical assessment of lattice-structured Onyx™ composites. Subsequently, structural parameters, including diameter and area, were evaluated. This sequence was designed based on specific technical criteria to ensure a comprehensive analysis.

2.5.1. Assessment of the diameter in lattice-structured composites.

The diameter of triangular planar Onyx™ compression composites was precisely measured using a vernier caliper with an accuracy of 0.01 mm. Additionally, CAD software was used to determine the theoretical diameter. Five separate measurements were taken for each composite, and their average was calculated to ensure accuracy. The diameter deviation (Dd) was then computed using the formula

$$Dd = Cd - Ad, \quad (2)$$

where Cd is the diameter obtained from CAD, and Ad is the actual measured diameter. This rigorous methodology ensured that the measurements were both reliable and accurate.

2.5.2. Assessment of the structural area in integrated lattice structures.

The structural area of integrated triangular planar lattice systems is measured using the ARCS KIM-U Video Measuring System, which is manufactured in India. This system measures the height and edge length of the lattice structures, with five measurements taken to compute the average values. Using these averages, the structural area is calculated with Equation 3:

Structural area of triangle = ½ (b ∗ h) (3)

where 'b' represents the base edge length and 'h' denotes the height of the triangular lattice structure. The difference in the structural area of the lattice structure is determined using Equation 4:

SAD = CSA - ASA (4)

Here, SAD stands for Structural Area Deviation, CSA represents the CAD Structural Area, and ASA is the Actual Structural Area. The CAD structural area is measured by evaluating the edge length and height with a measuring probe in the relevant CAD program, while the actual structural area is obtained through the VMS technique and Equation 3. This approach allows for the experimental evaluation of how MEX factors affect the structural accuracy of the integrated lattice structures.

2.6. Examining the fractures in the sample specimens.

Fracture modes observed during compression testing were captured using a Canon EOS 1500D DSLR camera, which offers 3x optical zoom, an 18 mm minimum focal length, 24.1 MP resolution, and 64 GB of storage. The recorded images of fracture modes were then analyzed to evaluate the effects of MEX factors, as detailed in Section 3.6. This comprehensive analysis provided valuable insights into how different MEX parameters influence the fracture behavior of the composites.

3. Results and discussion

3.1 Impact of MEX factors on the compressive strength of lattice-structured Onyx™ composites.

Figures 4 to 8 present a detailed analysis of how different material extrusion (MEX) parameters, specifically layer height, infill density, build orientation, infill pattern, and wall count, impact the compressive strength of lattice Onyx™ composites. These figures explore the effects of varying each parameter, offering insights into their role in determining the structural integrity and mechanical performance of the printed composites

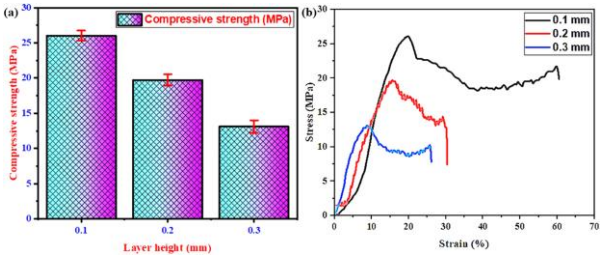

Fig. 4. Influence of layer height on the compressive strength of lattice-structured Onyx™ composites.

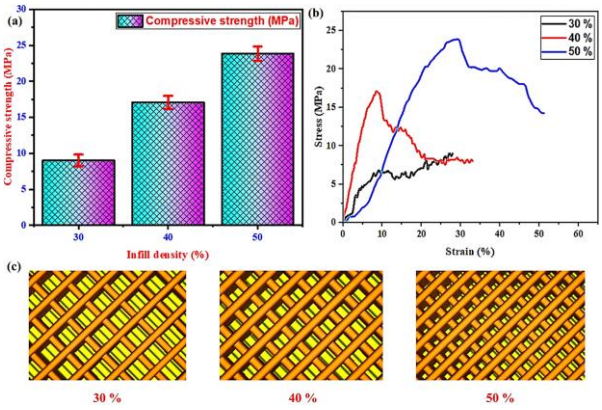

Fig. 5. Impact of infill density on the compressive strength of lattice-structured Onyx™ composites.

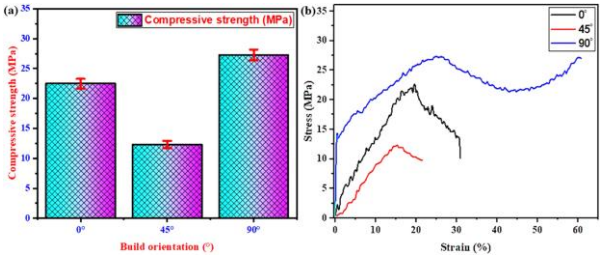

Fig. 6. Influence of build orientation on the compressive strength of lattice-structured Onyx™ composites.

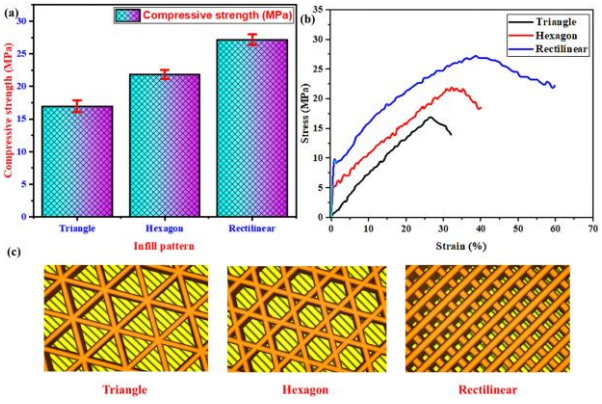

Fig. 7. Impact of infill pattern on the compressive strength of lattice-structured Onyx™ composites.

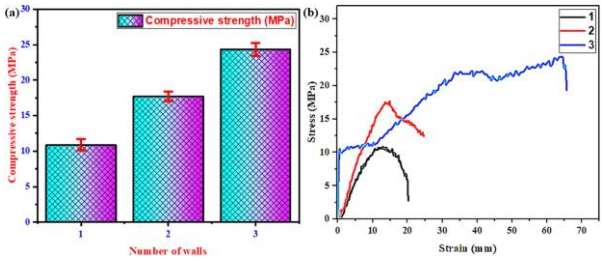

Fig. 8. Influence of the number of walls on the compressive strength of lattice-structured Onyx™ composites.

In Figure 4(a), the compression test outcomes are displayed, while Figure 4(b) depicts the stress-strain curves for lattice-structured Onyx™ composites produced with different layer heights of 0.1, 0.2, and 0.3 mm. The data demonstrates an inverse correlation between compressive strength and layer height. Specifically, a 0.1 mm layer height achieves the highest compressive strength, reaching 26.022 MPa. This increased strength is attributed to the higher number of layers, which reduces the rate of fracture propagation, thereby enhancing the overall structural integrity. On the other hand, as the layer height increases from 0.2 mm to 0.3 mm, the number of layers decreases, facilitating crack propagation and leading to earlier fractures. This results in lower compressive strengths of 19.725 MPa and 13.097 MPa, respectively.

Furthermore, composites with a 0.1 mm layer height exhibit the highest compressive modulus, which is linked to fewer defects and greater strain absorption during compression. This observation is consistent with the findings of Sikder et al., who reported that a 0.1 mm layer height in 3D printed PEEK components yielded a higher compressive strength of 106.45 MPa, due to the increased layer count in the vertical direction.

The experimental findings depicted in Figure 5(a) reveal the compressive strengths of lattice-structured Onyx™ composites, while Figure 5(b) showcases their stress-strain curves at varying infill densities of 30%, 40%, and 50%. The data clearly indicates that a 50% infill density leads to a substantial increase in compressive strength, reaching 23.831 MPa. This enhancement is due to the denser structure, which improves load-bearing capacity by minimizing the internal spacing between infill lines.

At lower infill densities, such as 30% and 40%, the compressive strengths are recorded at 9.022 MPa and 17.086 MPa, respectively. These lower densities result in wider spacing between infill lines, which creates air gaps that contribute to increased internal fractures and more rapid crack propagation.

Additionally, the 50% infill density not only achieves the highest compressive strength but also demonstrates the greatest strain at failure, signifying enhanced elongation and a higher compressive modulus. The finer and more intricate patterns produced by higher infill densities allow for better energy absorption, which contrasts with the performance of structures printed at lower infill densities. This behavior aligns with the observations made by Ma et al. in their study of cubic lattice materials.

Figure 6(b) illustrates the stress-strain curves of Onyx™ composites with lattice orientations at 0°, 45°, and 90°, while Figure 6(a) shows their respective compressive strengths. Among these, the composite with a 90° orientation demonstrated the highest compressive strength, reaching 27.279 MPa. This significant strength is due to the vertical arrangement of the composite layers, which buckle under compressive force with minimal lateral displacement, enhancing their load-bearing capacity.

In lattice-structured Onyx™ composites oriented at 0°, the layers are horizontally aligned with the axis of compressive stress during testing. This alignment leads to delamination, which reduces the compressive strength to 22.475 MPa. Composites oriented at 45° exhibit the weakest performance, with a compressive strength of just 12.306 MPa, due to layer displacement occurring early in the compression process. In contrast, composites with a 90° orientation show a higher compressive modulus, reaching a compressive strength of 27.279 MPa. This strength is attributed to the composite's progressive failure mechanisms. Similar fracture behaviors were reported by Mathiazhagan et al. in their study of

hydroxyapatite/PLA composite tubes with 0°, 45°, and 90° orientations.

Figure 7(a) displays the experimental compressive strengths, while Figure 7(b) illustrates the stress-strain curves for lattice-structured Onyx™ composites featuring hexagonal, triangular, and rectilinear infill patterns. Among these, the rectilinear infill pattern demonstrates the highest compressive strength at 27.172 MPa. In contrast, the triangular pattern exhibits the lowest compressive strength, measuring 16.962 MPa. The rectilinear pattern's superior strength is largely attributed to its ability to form lattice walls with higher infill densities, enhancing its structural integrity under compression.

In lattice-structured Onyx™ composites, hexagonal and triangular infill patterns are commonly used. However, these patterns often result in larger gaps between infill lines, which can contribute to increased fracture development and a decrease in compressive strength. Among these, the hexagonal pattern stands out due to its denser and more efficient packing, achieving a compressive strength of 21.851 MPa. In contrast, rectilinear infill patterns exhibit a higher density, enabling greater stretchability and a superior modulus of compression. Supporting evidence from Moreno-Núñez et al. highlights that incorporating carbon and glass fibers in a rectangular configuration significantly improves the mechanical properties of Onyx™/carbon fiber composites [43].

The experimental findings for lattice-structured Onyx™ composites, illustrated in Figures 8(a) and (b), present the compressive strength and stress-strain behavior for composites featuring one, two, and three walls. Among these, the composites with three walls demonstrated the highest compressive strength, reaching 24.339 MPa. These composites also exhibited prolonged resistance to compressive forces compared to those with fewer walls. Notably, composites with additional walls tend to undergo buckling fracture modes, which absorb more energy than delamination, leading to a higher compression modulus. The gradual failure through crushing observed in these composites further enhances this property. The optimal results were achieved with a layer height of 0.1 mm, a 50% infill density, a build orientation of 90°, a rectilinear infill pattern, and the incorporation of three walls.

3.2. The density of Onyx™ composites with a lattice structure is impacted by various Material Extrusion (MEX) factors.

Figure 9 explores the influence of several key factors on the density of Onyx™ composites with a lattice structure. These factors include wall count, build orientation, infill pattern, and layer height. The analysis provides a detailed examination of how each of these parameters contributes to the overall density of the composite material.

Figure 9(a) illustrates the density variations in lattice-structured components printed at different layer heights: 0.1 mm, 0.2 mm, and 0.3 mm. The experimental results show that a layer height of 0.1 mm yields the highest density at 0.0021 g/mm³, due to the greater material volume and cumulative layer weight. In comparison, components printed with layer heights of 0.2 mm and 0.3 mm exhibit lower densities, measuring 0.0005 g/mm³ and 0.0014 g/mm³, respectively.
Figure 9(b) shows the density differences in lattice-structured components at infill levels of 30%, 40%, and 50%. Components with 50% infill achieve a density of 0.0025 g/mm³, while those with 30% infill have a lower density of 0.0012 g/mm³.

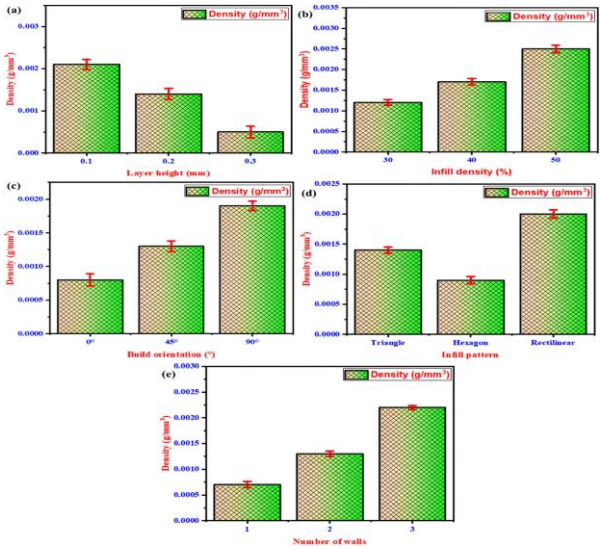

Fig. 9. The impact of (a) Layer height, (b) Infill density, (c) Build orientation, (d) Infill pattern, (e) Number of walls on the density of lattice-structured Onyx™ composites.

Lattice-structured composites with an infill density of 50% have more closely spaced infill lines compared to those with 30% or 40% infill density. This results in a denser internal structure, which improves the material's overall strength and stability. The increased number of infill lines at 50% density allows for a more even distribution of stress and load, making these composites ideal for applications that demand higher durability and resilience.

Figure 9 (C) highlights the density differences in lattice-structured Onyx™ composites printed at various orientations (0°, 45°, and 90°). Composites printed at a 90° orientation demonstrate the highest density of 0.0019 g/mm³, while those printed at a 0° orientation have the lowest density of 0.0008 g/mm³. The higher density observed in composites printed at 90° is attributed to the greater deposition of composite layers. In contrast, composites printed at a 45° orientation show a lower density of 0.0013 g/mm³ due to the reduced deposition of layers. This trend is similarly observed in composites printed at 0°. The density increases with the number of deposited layers, driven by the self-weight of the lattice structure under gravitational influence.

Figure 9(d) shows the experimental densities of lattice-structured Onyx™ composites with triangular, hexagonal, and rectilinear infill patterns. The rectilinear pattern yields a higher density of 0.002 g/mm³, compared to the hexagonal and triangular patterns, which have densities of 0.0009 g/mm³ and 0.0014 g/mm³, respectively. The rectilinear pattern achieves this by depositing infill lines laterally without creating internal porosities. In contrast, the hexagonal and triangular patterns result in internal porosities due to the way the infill lines are deposited, with the hexagonal pattern producing more porosities due to its larger morphological area. Consequently, increased internal porosity leads to lower densities in the composites.

Figure 9(e) illustrates the density variations in Onyx™ composites with different wall counts and lattice structures. The composite with three walls achieves the highest density of 0.0022 g/mm³, attributed to the increased lateral shelling provided by the additional circumferential walls. In contrast, composites with one or two walls display lower densities, following a different trend due to the reduced number of lateral shells. The relationship between wall count and density underscores the importance of wall thickness in achieving higher material density in lattice-structured composites.

The study identifies that the design configuration yielding the highest density features three walls, a 90° build orientation, 50% infill density, a 0.1 mm layer height, and a rectilinear infill pattern. In contrast, the lowest density is observed in a configuration with a single wall, 0° build orientation, 30% infill density, 0.3 mm layer height, and a hexagonal infill pattern. These findings highlight the significant impact of design parameters on the density of Onyx™ composites.

3.3 Impact of MEX factors on the diameter deviation of lattice-structured Onyx™ composites.

Figure 10 depicts the influence of different MEX parameters, such as layer height, infill density, build orientation, infill pattern, and wall count, on the diameter deviation of lattice-structured Onyx™ composites.

Figure 10(a) shows the diameter variations in lattice-structured Onyx™ composites at layer heights of 0.1 mm, 0.2 mm, and 0.3 mm. The smallest deviation of 0.116 mm is observed at a 0.1 mm layer height, while larger deviations of 0.328 mm and 0.415 mm occur at 0.2 mm and 0.3 mm, respectively. This trend is attributed to reduced splattering at the finer layer height of 0.1 mm, leading to better dimensional accuracy, while increased splattering at 0.2 mm and 0.3 mm results in greater deviations. This pattern is consistent with the findings of Chaidas et al., who noted that decreasing the layer height from 0.1 mm to 0.3 mm in PLA and PLA reinforced with wood flour similarly led to reduced dimensional accuracy in the X and Y orientations [44].

The diameter deviation of lattice-structured Onyx™ composites was assessed at infill densities of 30%,

40%, and 50%. The smallest variation, 0.162 mm, occurred at 50% infill density, suggesting improved printing accuracy as the print lines closely align with the geometric contour. In contrast, larger diameter deviations were noted at 30% and 40% infill densities, likely due to surface defects. This finding is consistent with Qattawi et al.'s study on PLA components, where thickness deviations increased with infill densities from 20% to 100%, while lower densities (20% and below) showed better accuracy and reduced shrinkage [45].

Figure 10(c) depicts the diameter deviation of lattice-structured Onyx™ composites printed at construction orientations of 0º, 45º, and 90º. The 90º orientation shows the smallest diameter deviation, at 0.125 mm, due to vertical layer deposition, which minimizes deviation and splattering. Conversely, larger diameter variations are observed at 45º and 0º orientations, where layers are deposited at inclined and horizontal angles, respectively.

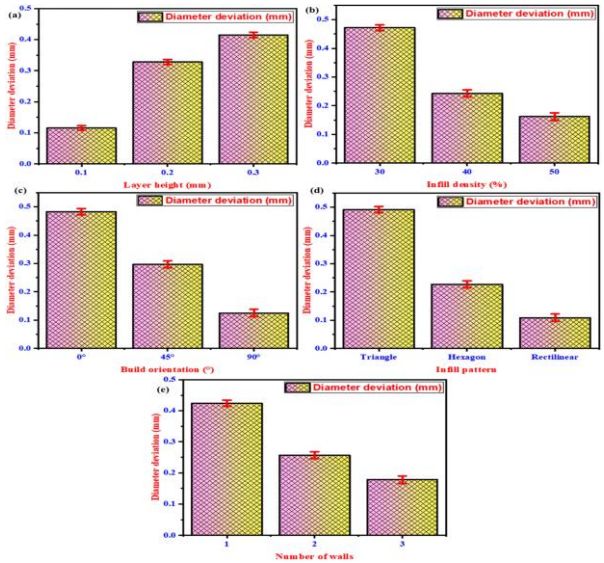

Fig. 10. The impact of (a) Layer height, (b) Infill density, (c) Build orientation, (d) Infill pattern, (e) Number of walls on the diameter deviation of lattice-structured Onyx™ composites.

When composite material is deposited at an angle rather than at a 90º orientation, it tends to accumulate along the curves of the geometric profile, resulting in greater diameter deviation. Similarly, horizontally placed material may sag or droop, leading to imperfections on the composite's lateral surface [46].

Figure 10(d) illustrates the diameter variation of lattice-structured Onyx™ composites with rectilinear, hexagonal, and triangular infill patterns. The rectilinear pattern, with closely spaced infill lines, produced the smallest deviation of 0.109 mm. In contrast, the triangular pattern, characterized by sharp vertices, resulted in larger fluctuations of 0.491 mm, while the hexagonal pattern showed a moderate deviation of 0.227 mm. Similar findings were reported by Qattawi et al. with PLA components, where triangular patterns exhibited greater deviation and rectilinear patterns showed minimal variation [45].

Figure 10(e) shows that the diameter deviation of lattice-structured OnyxTM composites decreases with increasing wall count. Composites with three walls have the smallest deviation (0.178 mm) due to better surface quality, while fewer walls lead to more defects and larger variations. This is consistent with previous studies on ABS composites, which found that multiple shells, especially three shells, improve accuracy compared to single-shell composites [47].

To minimize diameter variation, it is recommended to use a configuration with three walls, a rectilinear infill pattern, 50% infill density, a 90° build orientation, and a 0.1 mm layer height. This combination enhances dimensional accuracy by ensuring optimal material distribution and layer deposition.

3.4 Impact of MEX factors on the structural area deviation of integrated triangular lattice structures.

Figure 11 depicts the influence of several MEX parameters on the structural area deviation of lattice-structured Onyx™ composites. These parameters include layer height, infill density, build orientation, infill pattern, and wall count.

Figure 11(a) shows the structural area variation in integrated triangular lattice structures at different layer heights of 0.1, 0.2, and 0.3 mm. The highest structural area variation, reaching 0.432 mm², occurs at a 0.3 mm layer height due to the greater spreading of thicker composites during stacking. When the layer height is reduced to 0.2 mm and 0.1

mm, the structural area variation decreases to 0.225 mm² and 0.114 mm², respectively, reducing the potential for structural area mismatches [45].

Figure 11(b) presents the structural area variation in integrated lattice systems with infill densities of 30%, 40%, and 50%. At a 50% infill density, the structural area variation is minimized to 0.178 mm², owing to more uniform line deposition and fewer deviations in the lattice structure. In contrast, lowering the infill density to 30% and 40% increases the spacing between infill lines, leading to greater deviations in the lattice structure. Vidakis et al. observed similar results with ABS components, where raising the infill density from 80% to 100% improved the dimensional accuracy of printed parts [46].

Figure 11(c) illustrates the structural area deviation in integrated lattice structures across different build orientations of 0°, 45°, and 90°. A vertical build orientation (90°) significantly reduces structural area deviation, achieving a minimal deviation of 0.117 mm². In contrast, when the build orientation is horizontal (0°) or inclined at 45°, the lattice pores experience drooping and sagging, resulting in higher structural area deviations of 0.421 mm² and 0.279 mm², respectively.

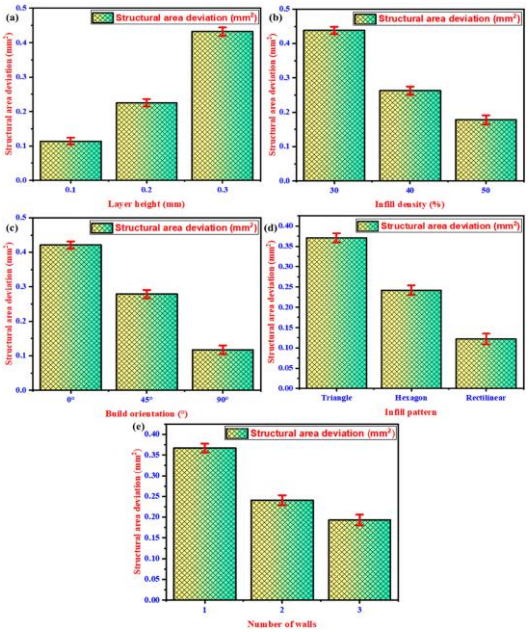

Fig. 11. The structural area deviation of integrated triangular lattice structures is influenced by (a) layer height, (b) infill density, (c) build orientation, (d) infill pattern, and (e) number of walls.

Figure 11(d) presents the structural area variation in integrated lattice systems using rectilinear, hexagonal, and triangular infill patterns. The rectilinear pattern demonstrates the smallest variation, measuring 0.122 mm², while the hexagonal and triangular patterns show greater variations at 0.242 mm² and 0.371 mm², respectively. The rectilinear design aligns more effectively within the lattice structure due to its consistent infill lines, whereas the hexagonal and triangular patterns face challenges due to their thinner walls. Qattawi et al. observed similar results with PLA components, where the triangular pattern had the highest structural area error, and the rectilinear pattern had the lowest [45].

Figure 11(e) illustrates the structural area deviation in integrated lattice systems with configurations of one, two, and three walls. The number of walls significantly impacts the structural area deviation along the lateral contour of the composite. The lowest deviation, at 0.193 mm², is observed with a three-wall configuration, while the highest deviation, at 0.367 mm², occurs with a single wall. Fewer walls lead to thinner configurations, causing greater lateral irregularities and structural area deviation in the triangular lattice structures. Jayashuriya et al. found similar results with ABS components, where using three walls at the boundary enhanced dimensional accuracy [47].

To minimize structural area deviation, an optimal configuration involves using three walls, a rectilinear infill pattern, a 50% infill density, a 90-degree build orientation, and a 0.1 mm layer height. This combination effectively reduces irregularities and enhances dimensional accuracy in lattice-structured composites.

3.5 Impact of MEX factors on the fracture patterns of lattice-structured Onyx™ composites

Figure 12 demonstrates the impact of different MEX parameters on the fractographic characteristics of lattice-structured Onyx™ composites. These parameters include layer height, infill density, build orientation, infill pattern, and wall count.

Figure 12(a) illustrates the fracture behaviors of Onyx™ composites with lattice structures at different layer heights, specifically 0.1 mm, 0.2 mm,

and 0.3 mm. Composites fabricated with 0.2 mm and 0.3 mm layer heights exhibit delayed crack propagation and buckling fractures, distinguishing them from those with a 0.1 mm layer height. Furthermore, when subjected to compressive stress, composites with 0.2 mm and 0.3 mm layer heights demonstrate layer separation, with the 0.3 mm samples showing a more pronounced degree of separation.

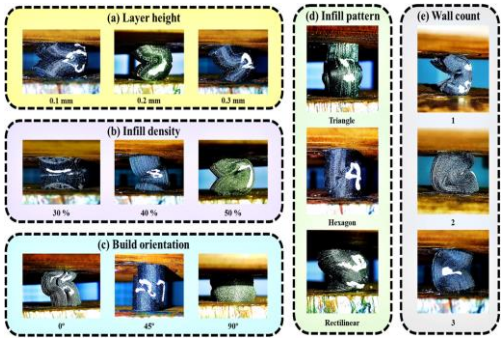

Fig. 12. Influence of (a) Layer height, (b) Infill density, (c) Build orientation, (d) Infill pattern, (e) Number of walls on the fracture characteristics of lattice-structured Onyx™ composites.

The fractography patterns of lattice-structured Onyx™ composites with different infill densities (30%, 40%, and 50%) are illustrated in Figure 12(b). Composites with 30% and 40% infill densities exhibit central fractures, while those with 50% or higher infill density demonstrate delayed crack growth and buckling fractures. Figure 12(c) presents the fractography modes of lattice-structured Onyx™ composites constructed at orientations of 0º, 45º, and 90º. Under compressive stress, composites with 0º layers begin to delaminate first, whereas those with a 45º orientation experience quicker layer slippage. Composites oriented at 90º exhibit increased tapping, leading to enhanced energy absorption.

Onyx™ composites with lattice structures display distinct fractography modes depending on the infill pattern used, such as rectilinear, hexagonal, and triangular. The rectilinear infill leads to buckling fractures, while triangular and hexagonal patterns cause slanted fractures and delamination, respectively. Figure 12(e) illustrates the fractography modes of lattice-structured Onyx™ composites with varying wall configurations—one, two, and three walls. Composites with more walls exhibit slower buckling, whereas those with fewer walls are prone to lateral delamination. The likelihood of delamination decreases as the number of walls increases, with three-walled lattice-structured Onyx™ composites showing the slowest buckling rate.

3.6. Comparison of the ideal combination with the standard Onyx™ composite.

In lattice-structured Onyx™ composites optimized with a Material Extrusion (MEX) factor, compressive loads are effectively dispersed throughout the lattice, leading to a gradual fracture process and increased strain percentages at a compressive strength of 36.95 MPa. This efficient load distribution contrasts with solid Onyx™ composites, which have a compressive strength of 197 MPa, aligning with previous findings by Fisher et al. [48]. The difference in compressive strength highlights the impact of lattice structuring on the material's mechanical performance, where the optimized lattice structure enhances strain capacity, while the solid structure provides superior compressive strength.

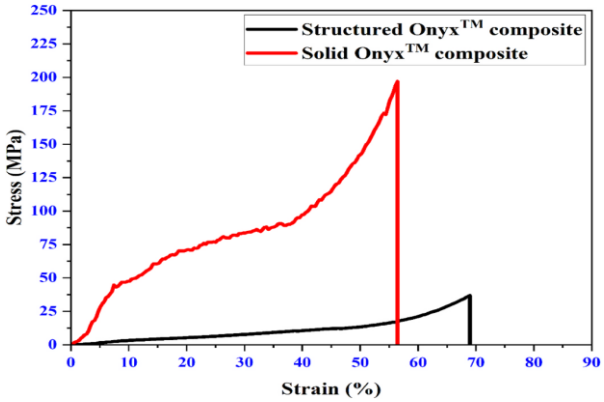

Fig. 13. depicts stress-strain curves for both solid and structured Onyx™ composites.

3.7 Uses of Onyx™ composites with honeycomb lattice structures.

In the rapidly advancing fields of photography and videography, both professionals and hobbyists are continually seeking new tools and methods to capture the perfect image. Among these tools, the L-bracket has seen a rise in popularity due to its ability to enhance stability and adaptability in camera systems. Initially designed for providing stability, L-brackets have become essential for achieving optimal camera performance. They allow photographers to easily switch between landscape

and portrait orientations, offering greater flexibility in composition and enabling precise framing from the outset.

Recent innovations in camera mounts have led to the introduction of lightweight yet durable polymers. While traditional brackets were often cumbersome and heavy, making them less practical for on-the-go use, newer designs now incorporate advanced materials such as carbon fiber reinforced polymers and aluminum alloys. These materials offer remarkable strength-to-weight ratios, providing both sturdiness and ease of transport. As a result, photographers can now enjoy longer shooting sessions with reduced fatigue, significantly enhancing both portability and overall convenience.

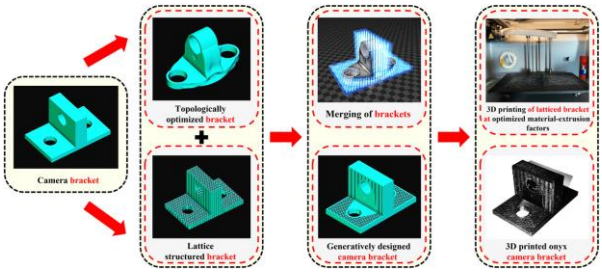

Fig 14 Steps involved in creating a lightweight Onyx™ camera bracket using a lattice structure.

Recently, the versatile OnyxTM composite material has found application in various fields, including housing components, sensor brackets, and mounts for portable cameras. Advanced manufacturing techniques allow for easy customization of components such as camera mounts. A recent study has utilized the OnyxTM material to fabricate lightweight, lattice-structured mounts for portable cameras like the GoPro.

The design process for lightweight camera brackets with a lattice construction involves several key steps. Initially, the bracket design is generated using nTopology software. Next, loads and constraints are applied to optimize the topology. To create a lightweight, load-bearing bracket, a triangular honeycomb unit cell lattice is integrated into the topologically optimized design. Constructed from OnyxTMcomposite material, the final bracket weighs 23% less than the original design. Mechanical strength is assessed through modeling, demonstrating a 15% efficiency gain over solid brackets. To achieve optimal results, the generatively designed bracket is printed using specific settings. Figure 14 illustrates the complete process of designing a lattice-structured OnyxTM camera bracket.

4. Conclusions

This study explores how various production settings influence the mechanical and physical properties of an innovative triangular honeycomb lattice structure made from a carbon-fiber reinforced Nylon composite. The findings reveal several key outcomes:

1. The integration of the triangular lattice structure is successfully achieved through carefully selected manufacturing parameters, which positively impact the overall quality of the composite.
2. Optimal compressive strength is achieved with a configuration that includes a 0.1 mm layer height, 50% infill density, a 90° construction orientation, a rectilinear infill pattern, and three walls. These settings are crucial for maximizing the composite's strength.
3. To achieve reduced density, the study found that using a 0.3 mm layer height, 30% infill density, 0° construction orientation, a hexagonal infill pattern, and a single wall is effective.
4. The study also identified that the lowest diameter and minimal structural area deviation are obtained with the same parameters that maximize compressive strength: 0.1 mm layer height, 50% infill density, 90° construction orientation, rectilinear infill pattern, and three walls.
5. The progressive tapping process applied to the composites leads to enhanced energy absorption in the lattice-structured Onyx™ when oriented at a 90° angle during construction.
6. Additionally, by combining topologically optimized designs with lattice-structured brackets, the study demonstrates the creation of stronger and lighter brackets. These brackets show a 23% reduction in weight and a 15% increase in mechanical strength, making them suitable for a range of applications, including preoperative surgical

planning and the 3D printing of medical instruments.

Data Availability

The study did not rely on any specific datasets.

Acknowledgment

The authors express their gratitude to the Researchers Supporting work, Saveetha Consortium for Future Technologies, Saveetha Engineering College, Saveetha Negar, Thandalam, Chennai - 602105, India.

Refrences

[1] Sharma D, Somashekhar S, & Hiremath SH. 'High-Temperature Creep Behavior of Selective-Laser-Melting-Fabricated Lattice Structures Inspired from Euplectella Aspergillum'. Advanced Engineering Materials, 26(3), 2024. doi:10.1002/adem.202301234.

[2] Sivakumar NK, Palaniyappan S, Basavarajappa S, Hashem MI, Bodaghi M, & Sekar V. 'Study on the impact of material extrusion factors on the compressive characteristics of honeycomb lattice-structured Onyx™ composites'. Materials Today Communications, 37 (2023) 107317. https://doi.org/10.1016/j.mtcomm.2023.107317.

[3] Mathiazhagan N, Sivakumar NK, Palaniyappan S, & Muthuramamoorthy M. 'A Topological Approach for Optimizing the Dimensional Properties of Various Bioinspired Periodic Type Honeycomb Latticed Carbon Fiber Reinforced Glycol-Modified Poly (Ethylene Terephthalate) Composite Materials'. Polymer Composites, 45(6) (2024) 5068-5083. https://doi.org/10.1002/pc.28110.

[4] Khan N, & Riccio A. 'A Systematic Review of Design for Additive Manufacturing of Aerospace Lattice Structures: Current Trends and Future Directions'. Progress in Aerospace Sciences, 149 (2024) 101021. doi:10.1016/j.paerosci.2024.101021.

[5] Mohammadi H, et al. 'An Insight from Nature: Honeycomb Pattern in Advanced Structural Design for Impact Energy Absorption'. Journal of Materials Research and Technology, 22 (2023) 2862-2887. https://doi.org/10.1016/j.jmrt.2022.12.063.

[6] Wei Y, Li H, Han J, et al. 'Mechanical and Damping Performances of TPMS Lattice Metamaterials Fabricated by Laser Powder Bed Fusion'. China Foundry, 21 (2024) 327-333. DOI: 10.1007/s41230-024-4026-5.

[7] Hu Q, Lu G, & Tse KM. 'Compressive and Tensile Behaviours of 3D Hybrid Auxetic-Honeycomb Lattice Structures'. International Journal of Mechanical Sciences, 263 (2024) article 108767. ISSN 0020-7403. DOI: 10.1016/j.ijmecsci.2023.108767.

[8] Sivakumar NK, Kaaviya J, Palaniyappan S, Nandhakumar GS, Prakash C, Basavarajappa S, Pandiaraj S, & Hashem MI. 'Machine Learning-Based Approach for Predicting the Compressive Strength of 3D Printed Hexagon Lattice-Cored Sandwich Structures'. Materials Today Communications, 110230 (2024). ISSN 2352-4928. DOI: 10.1016/j.mtcomm.2024.110230.

[9] Islam MA, Mobarak MH, Rimon MI, Mahmud ZA, Ghosh J, Ahmed MS, & Hossain N. 'Additive Manufacturing in Polymer Research: Advances, Synthesis, and Applications'. Polymer Testing, 132 (2024) 108364. ISSN 0142-9418. DOI: 10.1016/j.polymertesting.2024.108364.

[10] Ngo TD, Kashani A, Imbalzano G, Nguyen KTQ, & Hui D. 'Additive Manufacturing (3D Printing): A Review of Materials, Methods, Applications, and Challenges'. Composites Part B: Engineering, 143 (2018) 172-196. ISSN 1359-8368. DOI: 10.1016/j.compositesb.2018.02.012.

[11] Rayhan MT, Rimon MIH, Khan M, Hasan MA, Mobarak MH, Islam MA, & Hossain N. 'Advances in additive manufacturing of nanocomposite materials fabrications and applications'. European Polymer Journal, 113406 (2024). ISSN 0014-3057. DOI: 10.1016/j.eurpolymj.2024.113406.

[12] Kumar R, Singh R, Mehta A, Ranjan N, & Kumar V. 'On fused filament fabrication of PLA nanofiber reinforced PCL matrix-based smart porous scaffolds'. Materials Letters, 367 (2024)

136637. ISSN 0167-577X. DOI: 10.1016/j.matlet.2024.136637.

[13] Zhakeyev A, Devanathan R, & Marques-Hueso J. 'Modification of a Desktop FFF Printer via NIR Laser Addition for Upconversion 3D Printing'. HardwareX, 18 (2024) e00520. DOI:10.1016/j.ohx.2024.e00520.

[14] Ali RA, Karimi HR, & Mohamadi R. 'PLA-based Additively Manufactured Samples with Different Infill Percentages under Freeze-Thaw Cycles; Mechanical, Cracking, and Microstructure Characteristics'. Theoretical and Applied Mechanics Letters, 100536 (2024). https://doi.org/10.1016/j.taml.2024.100536.

[15] Bello I, Martínez-Abella F, Wardeh G, & González-Fonteboa B. 'Complete Stress-Strain Analysis of Masonry Prisms under Compressive Loading-Unloading Cycles through Digital Image Correlation'. Engineering Structures, 298 (2024) 117088. https://doi.org/10.1016/j.engstruct.2023.117088.

[16] Günaydın K, Rea C, & Kazancı Z. 'Energy Absorption Enhancement of Additively Manufactured Hexagonal and Re-Entrant (Auxetic) Lattice Structures by Using Multi-Material Reinforcements'. Additive Manufacturing, 59 part A (2022) 103076. ISSN 2214-8604. https://doi.org/10.1016/j.addma.2022.103076.

[17] Patro PK, Kandregula S, Khan MNS, & Das S. 'Investigation of Mechanical Properties of 3D Printed Sandwich Structures Using PLA and ABS'. Materials Today: Proceedings, 2023. https://doi.org/10.1016/j.matpr.2023.08.366.

[18] Mohan KT, Rao GB, Marshal JJ, Sudharvizhi M, Hindu M, Varsha G, Kumar KSC, Roshan KK, & Bannaravuri PK. 'Strengthening of Polymer Composites with an Addition of Ashoka Seeds and Eggshell Powder Particles'. Materials Today: Proceedings, 2024. https://doi.org/10.1016/j.matpr.2024.05.045.

[19] Khan T, Ali M, Riaz Z, Butt H, Abu Al-Rub RK, Dong Y, & Umer R. 'Recent Developments in Improving the Fracture Toughness of 3D-Printed Fiber-Reinforced Polymer Composites'. Composites Part B: Engineering, 283 (2024) 111622. https://doi.org/10.1016/j.compositesb.2024.111622.

[20] Cheng P, Li S, Peng Y, Le Duigou A, Wang K, & Ahzi S. '3D/4D Printed Functional Continuous Fiber-reinforced Polymer Composites: Progress and Perspectives'. Chinese Journal of Mechanical Engineering: Additive Manufacturing Frontiers, 2(3) (2023) 100090. https://doi.org/10.1016/j.cjmeam.2023.100090.

[21] Khan I, Tariq M, Abas M, Shakeel M, Hira F, Al Rashid A, & Koç M. 'Parametric Investigation and Optimisation of Mechanical Properties of Thick Tri-Material Based Composite of PLA-PETG-ABS 3D-Printed Using Fused Filament Fabrication'. Composites Part C: Open Access, 12 (2023) 100392. DOI:10.1016/j.jcomc.2023.100392.

[22] Tuli NT, Khatun S, & Rashid AB. 'Unlocking the Future of Precision Manufacturing: A Comprehensive Exploration of 3D Printing with Fiber-Reinforced Composites in Aerospace, Automotive, Medical, and Consumer Industries'. Heliyon, 10(5) (2024) e27328. DOI:10.1016/j.heliyon.2024.e27328.

[23] Buj-Corral I, & Zayas-Figueras EE. 'Comparative Study about Dimensional Accuracy and Form Errors of FFF Printed Spur Gears Using PLA and Nylon'. Polymer Testing, 117 (2023) 107862. DOI:10.1016/j.polymertesting.2022.107862.

[24] Yankin A, Serik G, Danenova S, Alipov Y, Temirgali A, Talamona D, & Perveen A. 'Optimization of fatigue performance of FDM ABS and nylon printed parts'. Micromachines, 14(2) (2023) 304.

[25] Makki T, Vattathurvalappil SH, Theravalappil R, Nazir A, Alhajeri A, Abdul Azeem M, Mahdi E, Ummer AC, & Ali U. '3D and 4D Printing: A Review of Virgin Polymers Used in Fused Deposition Modeling'. Composites Part C: Open Access, 14 (2024) 100472. https://doi.org/10.1016/j.jcomc.2024.100472.

[26] Ning F, Cong W, Qiu J, Wei J, & Wang S. 'Additive Manufacturing of Carbon Fiber Reinforced Thermoplastic Composites Using Fused Deposition Modeling'. Composites Part B: Engineering, 80 (2015) 369-378. ScienceDirect, https://doi.org/10.1016/j.compositesb.2015.06.013.

[27] Cococcetta NM, Pearl D, Jahan MP, & Ma J. 'Investigating Surface Finish, Burr Formation, and Tool Wear during Machining of 3D Printed Carbon Fiber Reinforced Polymer Composite'. Journal of Manufacturing Processes, 56B (2020) 1304-1316. https://doi.org/10.1016/j.jmapro.2020.04.025.

[28] Peng Y, Wu Y, Li S, Wang K, Yao S, Liu Z, & Garmestani H. 'Tailorable Rigidity and Energy-Absorption Capability of 3D Printed Continuous Carbon Fiber Reinforced Polyamide Composites'. Composites Science and Technology, 199 (2020) 108337. https://doi.org/10.1016/j.compscitech.2020.108337.

[29] Vidakis N, Petousis M, Velidakis E, Mountakis N, Grammatikos S, & Tzounis L. 'Multi-functional medical grade Polyamide12/Carbon black nanocomposites in material extrusion 3D printing'. Composite Structures, 311 (2023) 116788. ISSN 0263-8223. https://doi.org/10.1016/j.compstruct.2023.116788.

[30] Vidakis N, Petousis M, Velidakis E, Tzounis L, Mountakis N, Boura O, & Grammatikos SA. 'Multi-functional Polyamide 12 (PA12)/ Multiwall Carbon Nanotube 3D Printed Nanocomposites with Enhanced Mechanical and Electrical Properties'. Advanced Composite Materials, 31(6) (2022) 630-654. https://doi.org/10.1080/09243046.2022.2076019.

[31] Vellaisamy S, & Munusamy R. 'Experimental Study of 3D Printed Carbon Fibre Sandwich Structures for Lightweight Applications'. Defence Technology, 36 (2024) 71-77. https://doi.org/10.1016/j.dt.2023.11.019.

[32] Dubey D, Singh SP, & Behera BK. 'Review: Additive Manufacturing of Fiber-Reinforced Composites'. Journal of Materials Science, 59 (2024) 12219-12256. https://doi.org/10.1007/s10853-024-09925-6.

[33] Dong K, Wang Y, Wang Z, Qiu W, Zheng P, & Xiong Y. 'Reusability and Energy Absorption Behavior of 4D Printed Continuous Fiber-Reinforced Auxetic Composite Structures'. Composites Part A: Applied Science and Manufacturing, 169 (2023) 107529. https://doi.org/10.1016/j.compositesa.2023.107529.

[34] Jiang H, Jia R, Aiyiti W, Aihemaiti P, & Kasimu A. 'Infill Strategies for 3D-Printed CF-PEEK/HA-PEEK Honeycomb Core-Shell Composite Structures'. Journal of Manufacturing Processes, 92 (2023) 338-349. https://doi.org/10.1016/j.jmapro.2023.02.0

[35] Moreno-Núñez BA, Guerrero-Alvarado MA, Salgado-Castillo A, Treviño-Quintanilla CD, Cuan-Urquizo E, Sánchez-Santana U, & Pincheira-Orellana G. 'Build and Raster Orientation Effects on CFRP Onyx/Aramid Impact Absorption'. Composites Part C: Open Access, 14 (2024) 100485. https://doi.org/10.1016/j.jcomc.2024.100485.

[36] Ali Z, Yan Y, Mei H, Cheng L, & Zhang L. 'Effect of Infill Density, Build Direction and Heat Treatment on the Tensile Mechanical Properties of 3D-Printed Carbon-Fiber Nylon Composites'. Composite Structures, 304(1) (2023) 116370. DOI:10.1016/j.compstruct.2022.116370.

[37] Nikiema D, Sène NA, Balland P, & Sergent A. 'Study of Walls' Influence on the Mechanical Properties of 3D-Printed Onyx Parts: Experimental, Analytical and Numerical Investigations'. Heliyon, 9(8) (2023) e19187. DOI:10.1016/j.heliyon.2023.e19187.

[38] Vijayakumar MD, Palaniyappan S, Veeman D, & Tamilselvan M. 'Process optimization of hexagonally structured polyethylene terephthalate glycol and carbon fiber composite with added shell walls'. Journal of Materials Engineering and Performance, (2022) 1–14.

[39] Gong P, Hao L, Li Y, Li Z, & Xiong W. '3D-printed carbon fiber/polyamide-based flexible honeycomb structural absorber for multifunctional broadband microwave absorption'. Carbon, 185 (2021) 272–281.

[40] Sikder P, Challa BT, & Gummadi SK. 'A comprehensive analysis on the processing-structure-property relationships of FDM-based 3-D printed polyetheretherketone (PEEK) structures'. Materialia, 22 (2022) 101427.

[41] Ma Q, Rejab MRM, Kumar AP, Fu H, Kumar NM, & Tang J. 'Effect of infill pattern, density and material type of 3D printed cubic structure under quasi-static loading'. Proceedings of the Institution of Mechanical Engineers, Part C: Journal of Mechanical Engineering Science, 235(19) (2021) 4254–4272.

[42] Mathiazhagan N, Palaniyappan S, & Sivakumar NK. 'Effect of fused filament fabrication parameters on crashworthiness studies of hydroxyapatite particle reinforced PLA composite thin-walled tubes'. Journal of Mechanical Behavior of Biomedical Materials, 138 (2023) 105611.

[43] Moreno-Núñez BA, Abarca-Vidal CG, Treviño-Quintanilla CD, Sánchez-Santana U, Cuan-Urquizo E, & Uribe-Lam E. 'Experimental analysis of fiber reinforcement rings' effect on tensile and flexural properties of Onyx™–Kevlar® composites manufactured by continuous fiber reinforcement'. Polymers, 15(5) (2023) 1252.

[44] Chaidas D, & Kechagias JD. 'An investigation of PLA/W parts quality fabricated by FFF'. Materials and Manufacturing Processes, 37(5) (2022) 582–590.

[45] Qattawi A. 'Investigating the effect of fused deposition modeling processing parameters using Taguchi design of experiment method'. Journal of Manufacturing Processes, 36 (2018) 164–174.

[46] Vidakis N, David C, Petousis M, Sagris D, & Bracketakis N. 'Optimization of key quality indicators in material extrusion 3D printing of acrylonitrile butadiene styrene: The impact of critical process control parameters on the surface roughness, dimensional accuracy, and porosity'. Materials Today Communications, 34 (2023) 105171.

[47] Jayashuriya M, Gautam S, Aravinth AN, Vasanth G, & Murugan R. 'Studies on the effect of part geometry and process parameter on the dimensional deviation of additive manufactured part using ABS material'. Progress in Additive Manufacturing, (2022) 1–11.

[48] Fisher T, Almeida JHS Jr, Falzon BG, & Kazancı Z. 'Tension and compression properties of 3D-printed composites: print orientation and strain rate effects'. Polymers, 15(7) (2023) 1708.

Bibliographic

Dr. S. Sellakumar was born on March 26, 1986. He completed his Bachelor of Engineering in Mechanical Engineering from Saveetha Engineering College, Anna University, Chennai, in 2007, and his Master of Engineering in CAD/CAM from Kongu Engineering College, Anna University, Coimbatore, in 2010. He obtained his Ph.D. in Mechanical Engineering from Anna University, Chennai, in 2020.

He has 14 years of academic experience as an Assistant Professor at Saveetha Engineering College, Chennai, India. His research interests include Computer Applications in Design, Reverse Engineering, Additive Manufacturing, and Finite Element Analysis.

Email: sellakumar.s@gmail.com